

## Part II, 3. Energy measurement in calorimeters

3.1 Concept of a calorimeter in particle physics

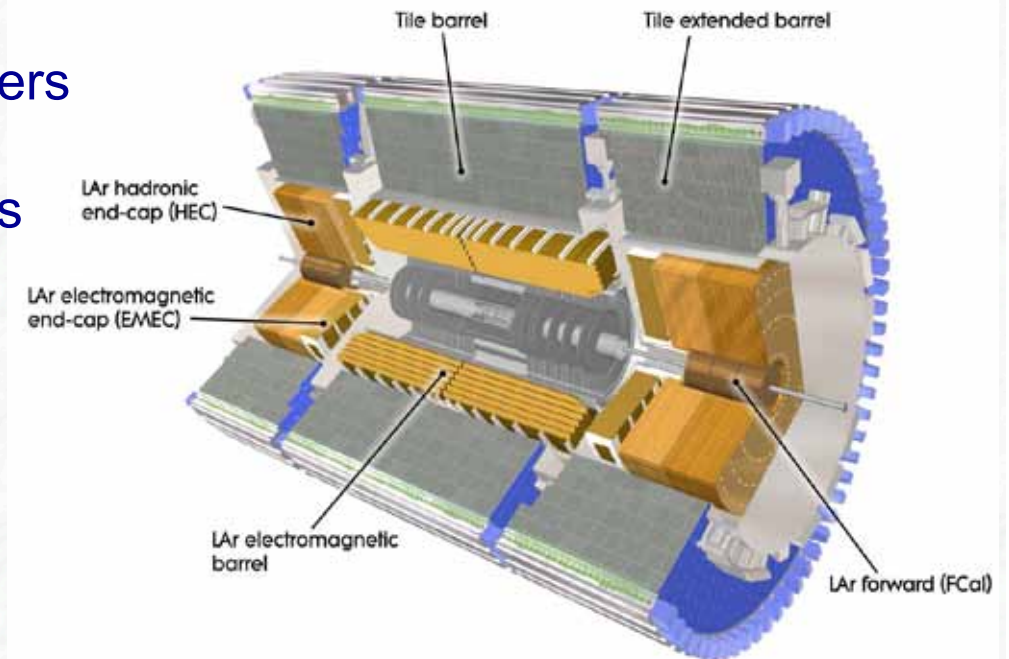
3.2 Interactions of photons with matter

3.3 Electromagnetic and hadronic showers

3.4 Layout and readout of calorimeters

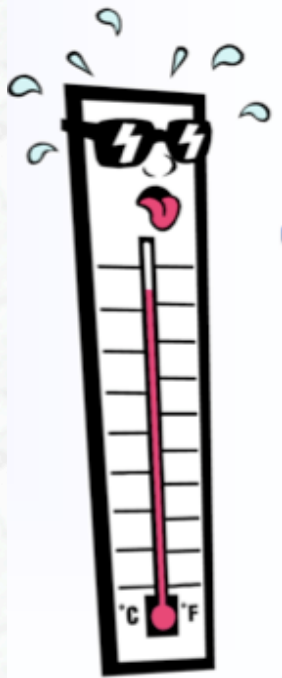
3.5 Energy resolution in calorimeters

3.6 The ATLAS and CMS calorimeter systems



Calorimetry: = Energy measurement by total absorption,  
usually combined with spatial information / reconstruction

*latin: calor = heat*



However: calorimetry in particle physics does not correspond to measurements of  $\Delta T$

- The temperature change of 1 liter water at 20 °C by the energy deposition of a 1 GeV particle is  $3.8 \cdot 10^{-14}$  K !
- LHC: total stored beam energy  
 $E = 10^{14}$  protons  $\cdot$  14 TeV  $\sim 10^8$  J

If transferred to heat, this energy would only suffice to heat a mass of 239 kg water from 0° to 100°C

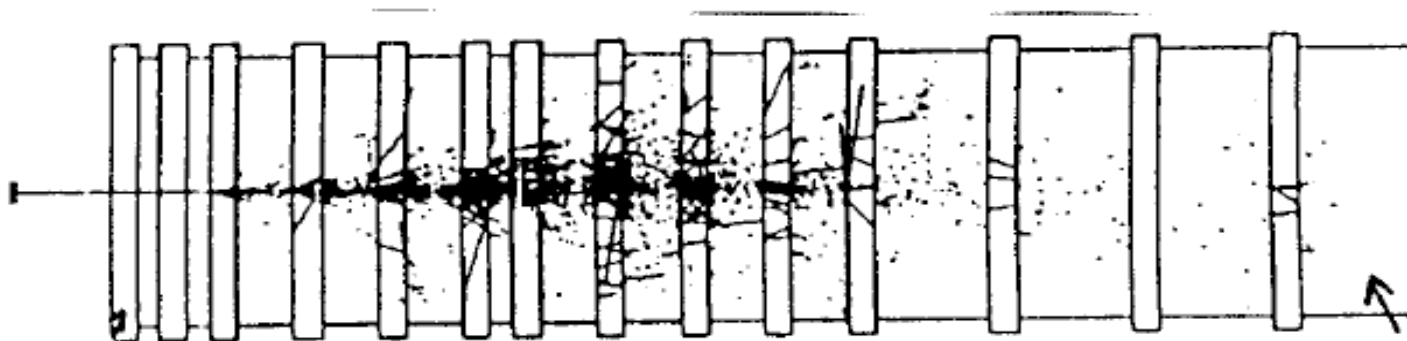
$$[c_{\text{Water}} = 4.18 \text{ J g}^{-1} \text{ K}^{-1}, \quad m = \Delta E / (c_{\text{Water}} \Delta T ) ]$$

## 3.1 Concept of a calorimeter in particle physics

- Primary task: measurement of the total **energy of particles**
- Energy is transferred to an **electrical signal** (ionization charge) or to a **light signal** (scintillators, Cherenkov light)  
This **signal** should be **proportional to the original energy**:  $E = \alpha S$   
**Calibration procedure**  $\rightarrow \alpha$  [GeV / S]

Energy of primary particle is transferred to new, particles,  
 $\rightarrow$  cascade of new, lower energy particles

- Layout: block of material in which the particle deposits its energy  
(absorber material (Fe, Pb, Cu,...))  
+ sensitive medium (Liquid argon, scintillators, gas ionization detectors,..)



## Important parameters of a calorimeter:

- **Linearity** of the energy measurement
- Precision of the energy measurement (**resolution**,  $\Delta E / E$ )  
in general limited by fluctuations in the shower process

worse for sampling calorimeters as compared to homogeneous calorimeters

- Uniformity of the energy response to different particles (**e/h response**)  
in general: response of calorimeters is different to so called electromagnetic particles (e,  $\gamma$ ) and hadrons (h)

# Overview of interaction processes of electrons and photons

Energy loss due to excitation and ionisation

Bethe Bloch formula

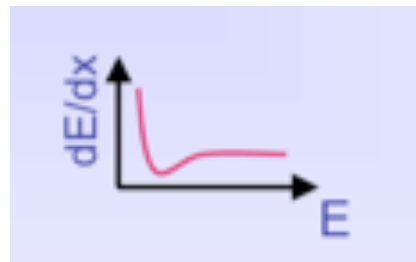
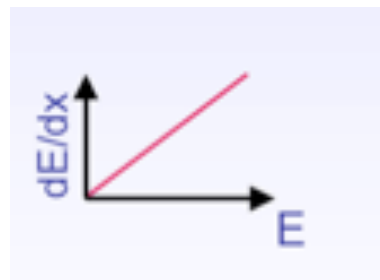


Photo effect

(dominant in  $\sim$  keV energy range)



Bremsstrahlung



Compton effect

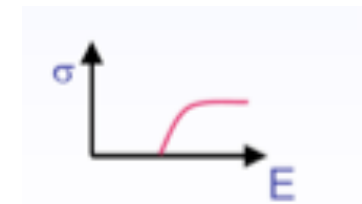
(dominant in MeV energy range)



Cherenkov radiation

Pair creation

(threshold energy =  $2 m_e = 1,022$  MeV)



## 3.2 Interactions of photons with matter

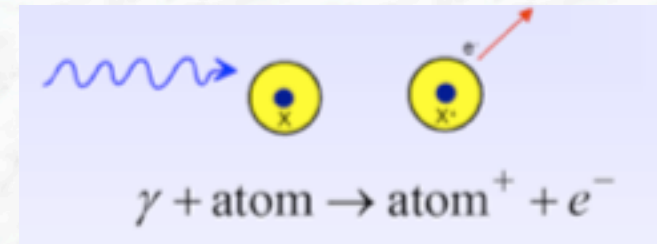
In order to be detected, photons must transfer their energy to charged particles

- Photo electric effect
- Compton scattering
- Pair creation

Photons “disappear” via these reactions. The Intensity of a photon beam is exponentially attenuated in matter:

$$I(x) = I_0 e^{-\mu x}$$

## Photo electric effect:



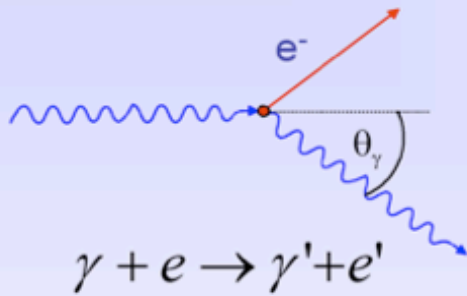
- Release of electrons from the inner shells (K, L, ..) of atoms  
(Only possible in the close neighbourhood of a third collision partner)
- The cross section shows a strong modulation if  $E_\gamma \approx E_{\text{bin}}$  (binding energy)

$$\sigma_{photo}^K = \left(\frac{32}{\varepsilon^7}\right)^{\frac{1}{2}} \alpha^4 Z^5 \sigma_{Th}^e \quad \varepsilon = \frac{E_\gamma}{m_e c^2} \quad \sigma_{Th}^e = \frac{8}{3} \pi r_e^2 \quad (\text{Thomson})$$

At high energies ( $\varepsilon \gg 1$ )

$$\sigma_{photo}^K = 4\pi r_e^2 \alpha^4 Z^5 \frac{1}{\varepsilon} \quad \boxed{\sigma_{photo} \propto Z^5}$$

# Compton scattering:



$$E'_\gamma = E_\gamma \frac{1}{1 + \varepsilon(1 - \cos\theta_\gamma)}$$

$$E_e = E_\gamma - E'_\gamma$$

Assume electron as quasi-free.

**Klein-Nishina**  $\frac{d\sigma}{d\Omega}(\theta, \varepsilon)$   $\rightarrow$

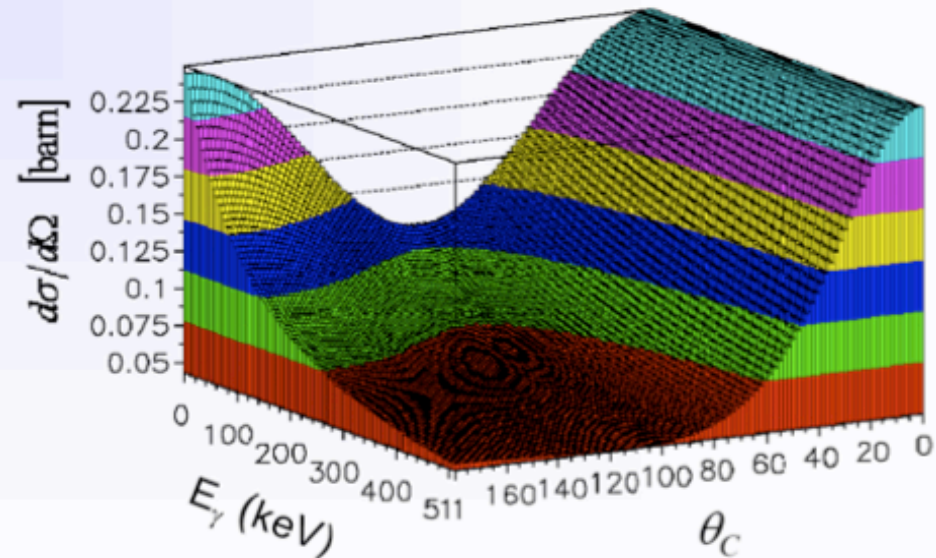
At high energies approximately

$$\sigma_c^e \propto \frac{\ln \varepsilon}{\varepsilon}$$

Atomic Compton cross-section:

$$\sigma_c^{atomic} = Z \cdot \sigma_c^e$$

Compton cross-section (Klein-Nishina)



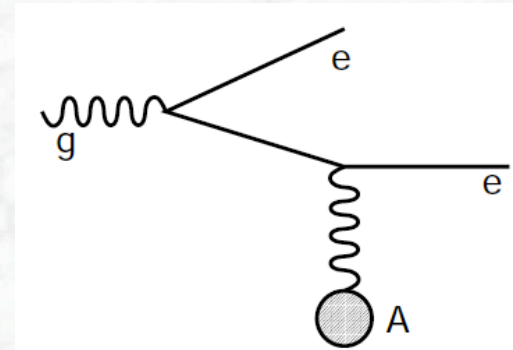
## Pair production: $\gamma + (A) \rightarrow e^+ e^- + (A)$

- Only possible in the close neighbourhood of a collision partner (atomic nucleus)
- Threshold energy:  $E_\gamma > 2 m_e c^2 = 1.022 \text{ MeV}$
- Cross section (high energy approximation):

$$\sigma_{pair} = 4\alpha r_e^2 Z^2 \left( \frac{7}{9} \ln \frac{183}{Z^{1/3}} - \frac{1}{54} \right) \approx \frac{7}{9} \frac{A}{N_A} \frac{1}{X_0}$$



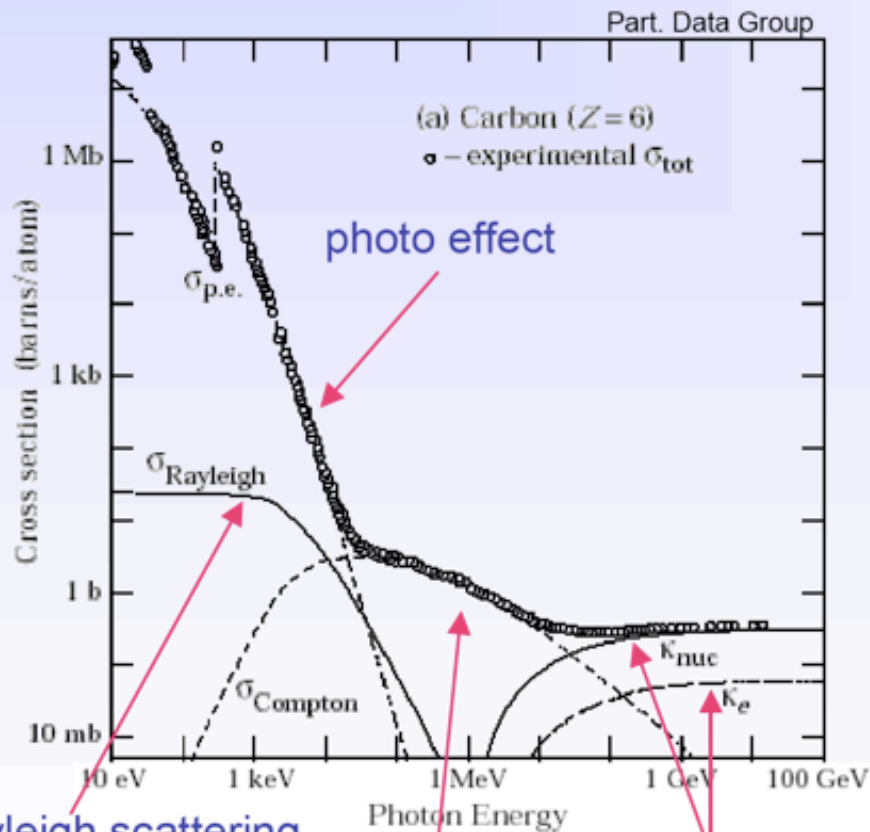
$$\mu_{pair} = \frac{7}{9} \frac{1}{X_0}$$



- After traversing a material thickness of  $9/7 X_0$ , the photon intensity –due to pair creation- is decreased by  $1/e$   
.or.
- For high photon energies, pair production occurs after traversing a material thickness corresponding to one radiation length with a probability of

$$p = 1 - e^{-7/9} = 0.54$$

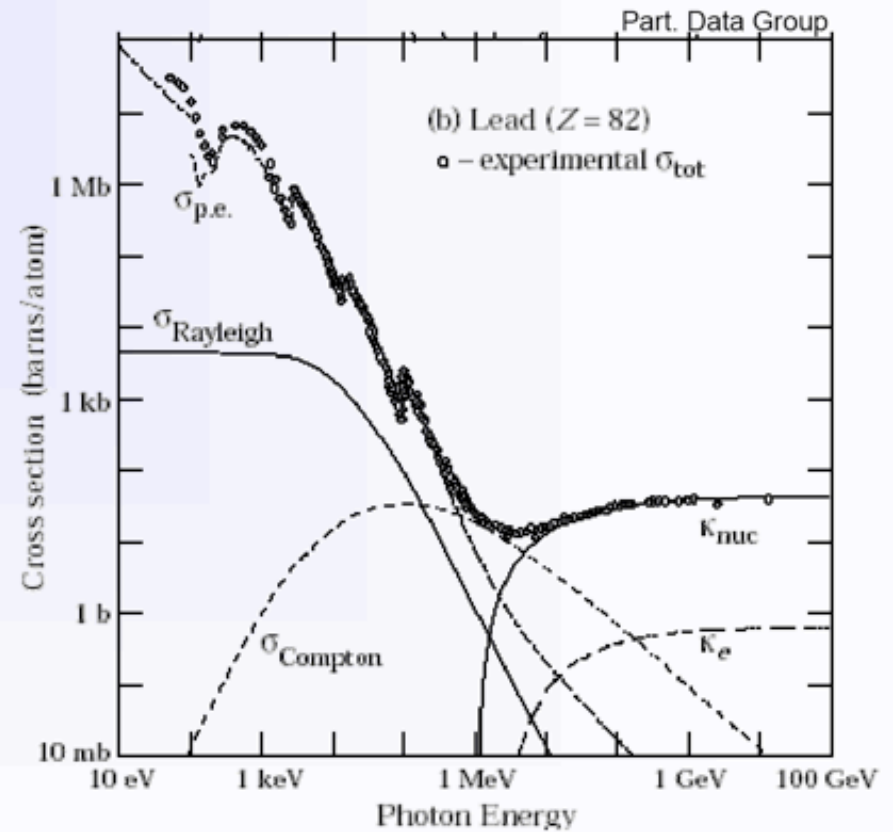
# Photon interaction cross sections



Rayleigh scattering  
(no energy loss !)

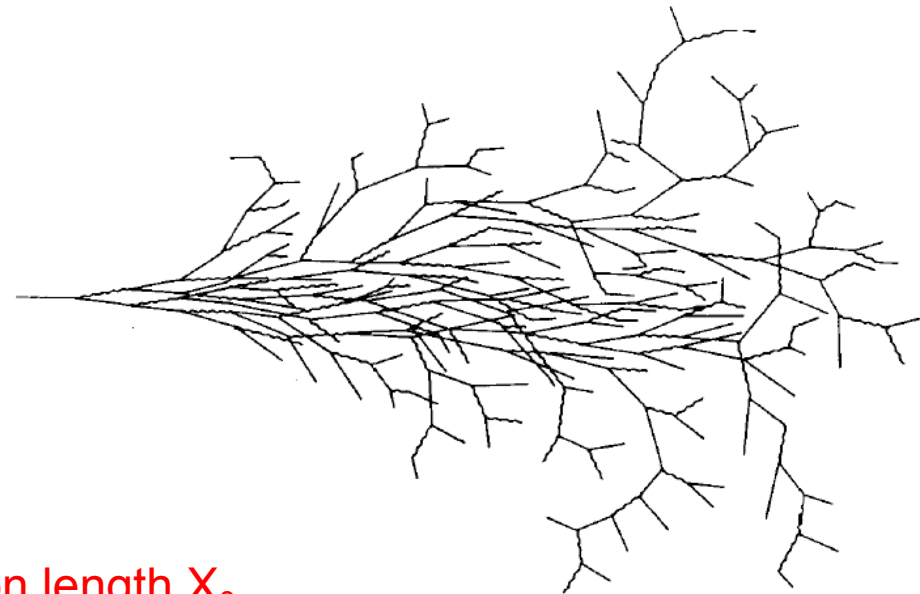
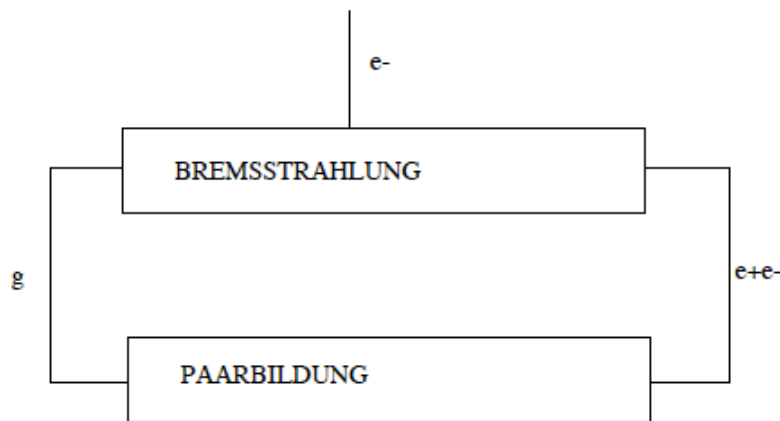
Compton scattering

pair production



## 3.3 Electromagnetic showers

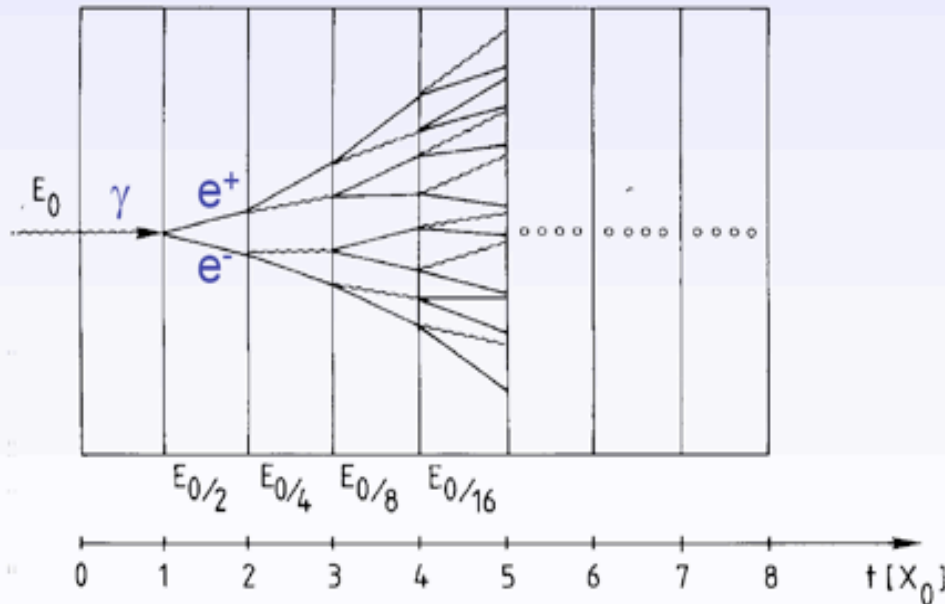
- Particle showers created by electrons/positrons or photons are called electromagnetic showers (only electromagnetic interaction involved)
- Basic processes for particle creation: bremsstrahlung and pair creation



- Characteristic interaction length: radiation length  $X_0$
- Number of particles in the shower increases, until the critical energy  $E_c$  is reached; For  $E < E_c$  the energy loss due to ionization and excitation dominates, the number of particles decreases, due to stopping in material

# Longitudinal shower profile

## Simple qualitative model



- Consider only **Bremsstrahlung** and (symmetric) **pair production**.
- Assume:  $X_0 \sim \lambda_{\text{pair}}$

$$N(t) = 2^t \quad E(t)/\text{particle} = E_0 \cdot 2^{-t}$$

Process continues until  $E(t) < E_c$

$$N^{\text{total}} = \sum_{t=0}^{t_{\text{max}}} 2^t = 2^{(t_{\text{max}}+1)} - 1 \approx 2 \cdot 2^{t_{\text{max}}} = 2 \frac{E_0}{E_c}$$

$$t_{\text{max}} = \frac{\ln E_0 / E_c}{\ln 2}$$

After  $t = t_{\text{max}}$  the dominating processes are **ionization, Compton effect and photo effect absorption of energy**.

Shower depth (shower maximum) scales logarithmically with particle energy !

→ size of calorimeters growth only logarithmically with energy.

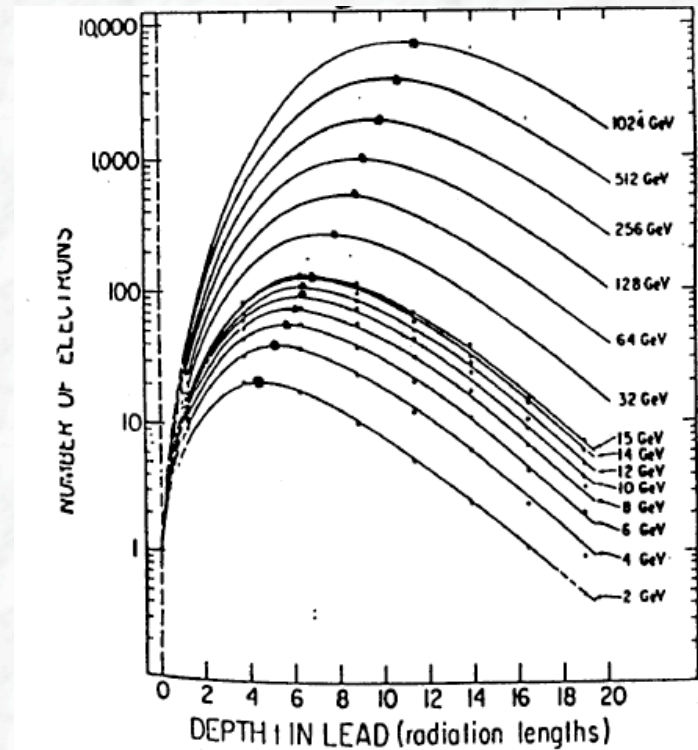
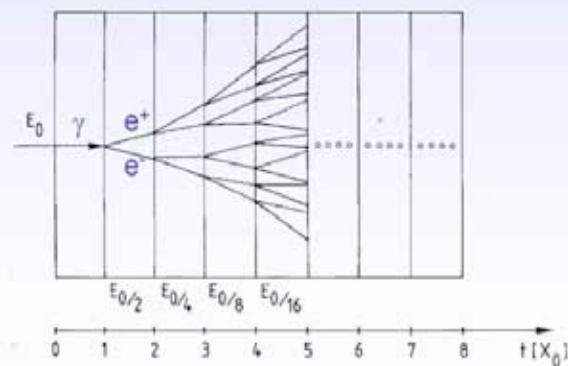
# Longitudinal shower parametrization ( $t [X_0]$ = thickness in units of $X_0$ )

$$\frac{dE}{dt} = \text{const} \cdot t^a \cdot e^{-bt}$$

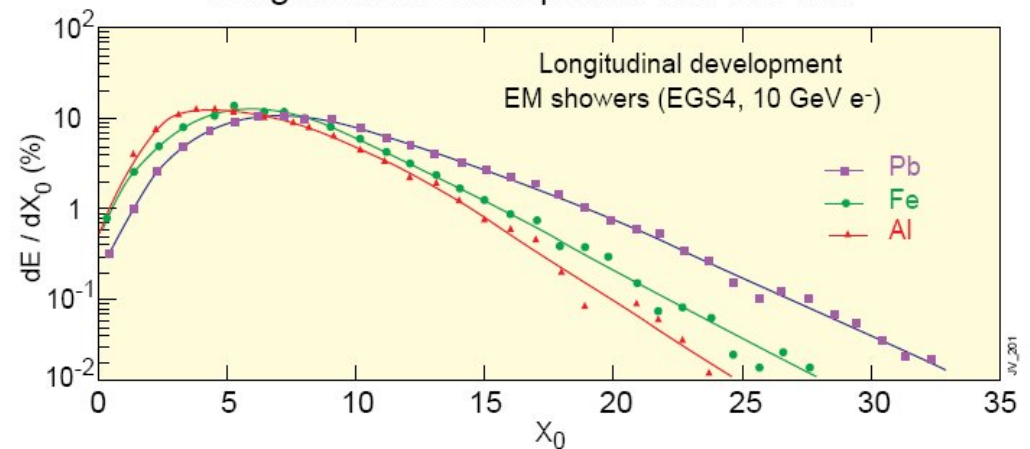
Shower depth (shower maximum) scales logarithmically with particle energy !

→ size of calorimeters growth only logarithmically with energy.

can be derived using a simple shower model (see exercises)



Longitudinal Development EM Shower



## Lateral shower profile:

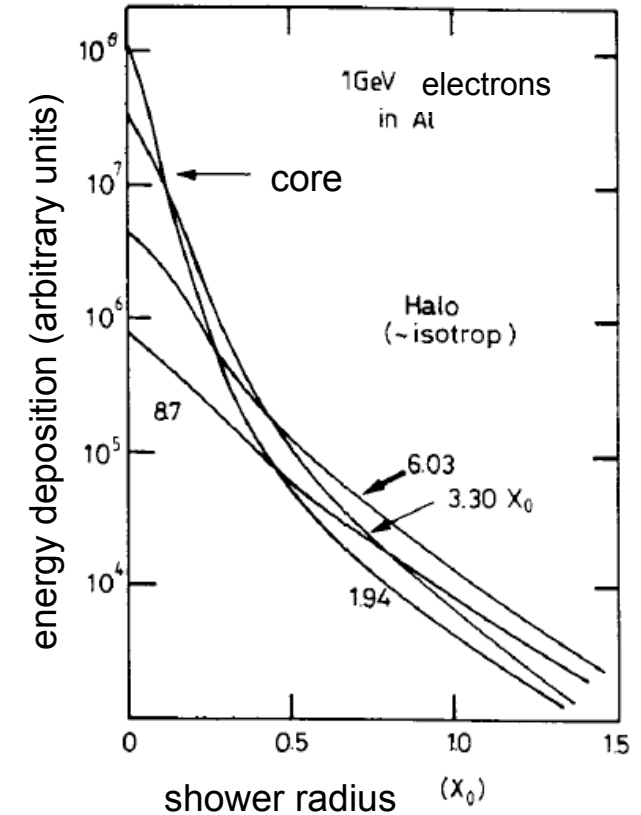
- The lateral shower profile is dominated by two processes:
  - Multiple Coulomb scattering
  - Relatively long free path length of low energy photons

- It is characterized by the so-called Molière radius  $\rho_M$

$$\rho_M = \frac{21\text{MeV}}{E_C} X_0 \approx 7 \frac{A}{Z} \left[ \frac{g}{\text{cm}^2} \right]$$

- About 95% of the shower energy are contained within a cylinder with radius  $r = 2 \rho_M$

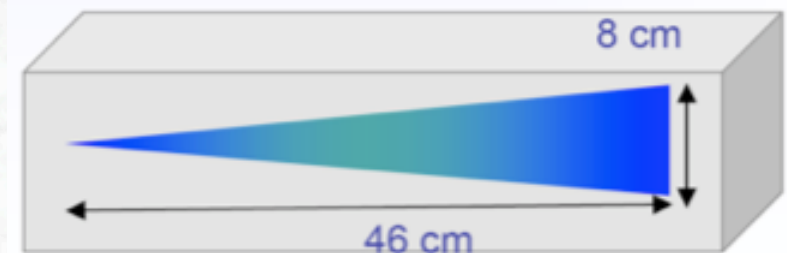
in general well collimated !



Example:  $E_0 = 100$  GeV in lead glass

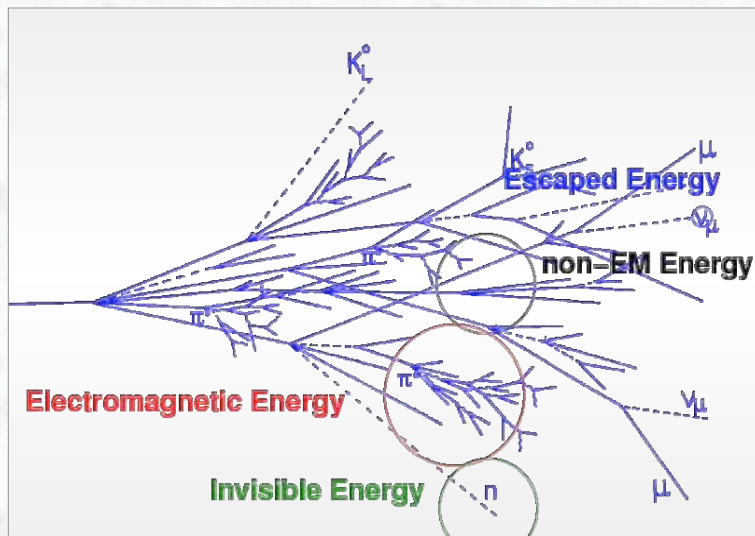
$E_C = 11.8$  MeV  $\rightarrow I_{max} \approx 13$ ,  $I_{95\%} \approx 23$

$X_0 \approx 2$  cm,  $R_M = 1.8 \cdot X_0 \approx 3.6$  cm



# Hadronic showers

- Hadrons initiate their energy shower by inelastic hadronic interactions; (strong interaction responsible, showers are called **hadronic showers**)
- Hadronic showers are much more complex than electromagnetic showers



- Several secondary particles, meson production, multiplicity  $\sim \ln(E)$
- $\pi^0$  components,  $\pi^0 \rightarrow \gamma\gamma$ , **electromagnetic sub-showers**;  
The fraction of the electromagnetic component grows with energy,  
 $f_{EM} = 0.1 \ln E$  (E in GeV, in the range  $10 \text{ GeV} < E < 100 \text{ GeV}$ )

- During the hadronic interactions atomic nuclei are broken up or remain in excited states

Corresponding energy (excitation energy, binding energy) comes from original particle energy

→ no or only partial contribution to the visible energy

- In addition, there is an important neutron component

The interaction of neutrons depends strongly on their energy;

Extreme cases:

- Nuclear reaction, e.g. nuclear fission → energy recovered
- Escaping the calorimeter (undergo only elastic scattering, without inelastic interaction)

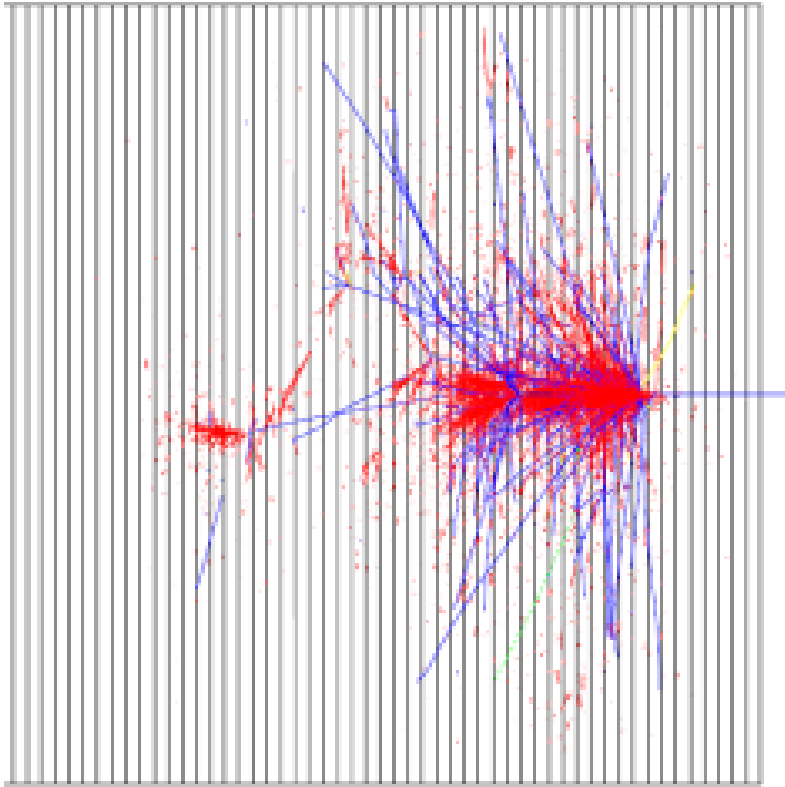
- Decays of particles (slow particles at the end of the shower)

e.g.  $\pi \rightarrow \mu \nu_\mu$  → escaping particles → missing energy

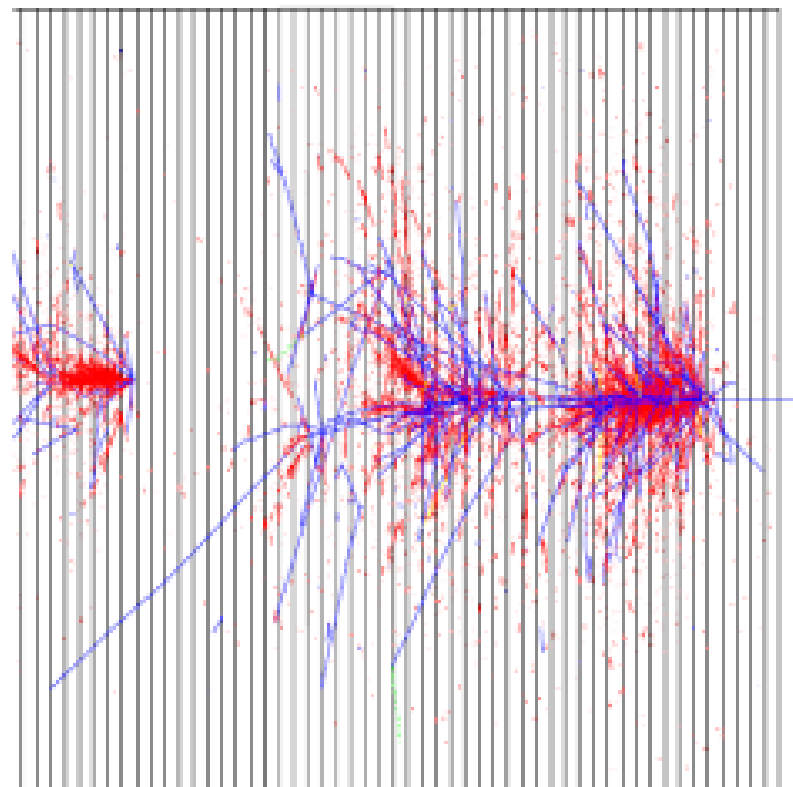
These energy loss processes have important consequences:  
in general, the response of the calorimeter to electrons/photons and hadrons is different ! The signal for hadrons is non-linear and smaller than the e/ $\gamma$  signal for the same particle energy

## Two hadronic showers in a sampling calorimeter

1.



2.



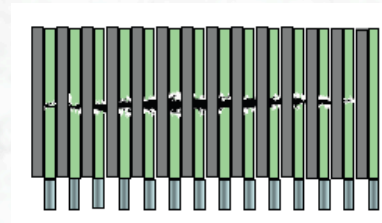
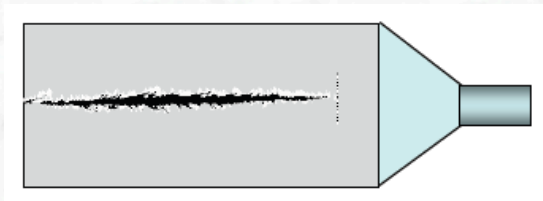
Red: electromagnetic component  
Blue: charged hadron component

Hadronic showers show very large fluctuations from one event to another  
→ the energy resolution is worse than for electromagnetic showers

## 3.4 Layout and readout of calorimeters

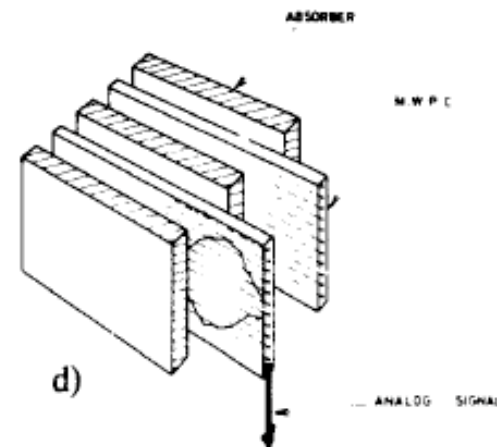
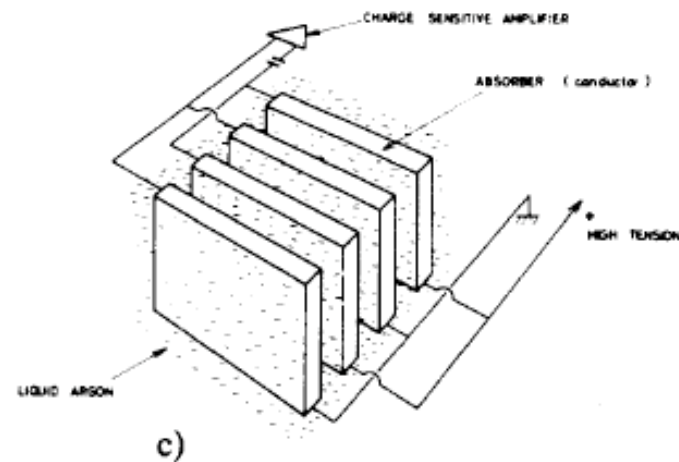
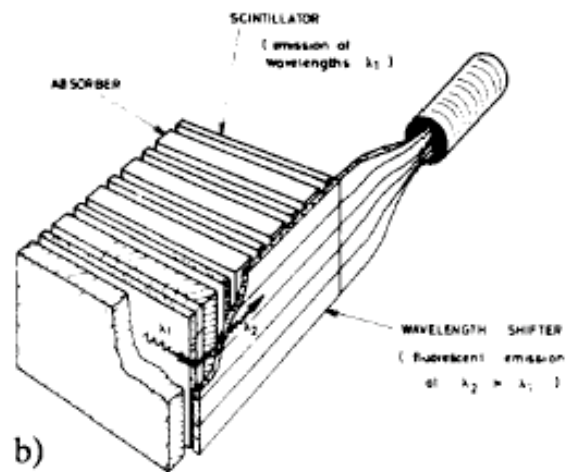
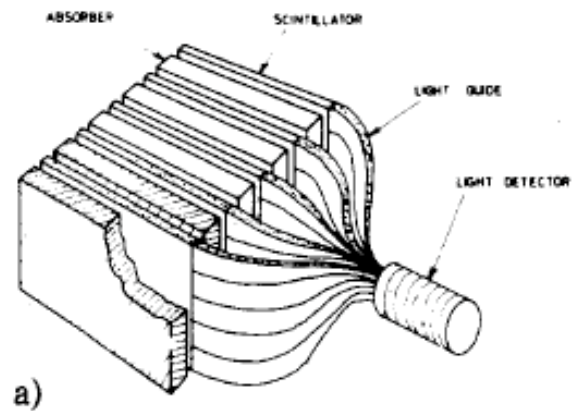
- In general, one distinguishes between **homogenous calorimeters** and **sampling calorimeters**

**For homogeneous calorimeters:** absorber material = active (sensitive) medium



- Examples for **homogeneous calorimeters**:
  - NaJ or other crystals (Scintillation light)
  - Lead glass (Cherenkov light)
  - Liquid argon or liquid krypton calorimeters (Ionization charge)
- **Sampling calorimeters**: absorption and hadronic interactions occur mainly in dedicated absorber materials (dense materials with high Z, passive material)  
Signal is created in active medium, only a fraction of the energy contributes to the measured energy signal

## Examples for sampling calorimeters



- (a) Scintillators, optically coupled to photomultipliers
- (b) Scintillators, wave length shifters, light guides
- (c) Ionization charge in liquids
- (d) Ionization charge in multi-wire proportional chambers

## 3.5 Energy resolution of calorimeters

- The energy resolution of calorimeters depends on the fluctuations of the measured signal (for the same energy  $E_0$ ),  
i.e. on the fluctuation of the measured signal delivered by charged particles.

Example: Liquid argon, ionization charge:  $Q = \langle N \rangle \langle T_0 \rangle \sim E_0$   
where:  $\langle N \rangle$  = average number of produced charge particles,  
 $\sim E_0 / E_c$   
 $\langle T_0 \rangle$  = average track length in the active medium

For sampling calorimeters only a fraction  $f$  of the total track length  
(the one in the active medium) is relevant;  
Likewise, if there is a threshold for detection (e.g. Cherenkov light)

- The energy resolution is determined by statistical fluctuations:
  - Number of produced charged particles (electrons for electromagnetic showers)
  - Fluctuations in the energy loss (Landau distribution of Bethe-Bloch sampling)

- For the resolution one obtains: 
$$\frac{\Delta E}{E} = \frac{\Delta Q}{Q} \propto \frac{\sqrt{N}}{N} \propto \frac{\alpha}{\sqrt{E}}$$

- The energy resolution of calorimeters can be parametrized as:

$$\frac{\Delta E}{E} = \frac{\alpha}{\sqrt{E}} \oplus \beta \oplus \frac{\gamma}{E}$$

- $\alpha$  is the so called **stochastic term** (statistical fluctuations)
- $\beta$  is the **constant term** (dominates at high energies)

important contributions to  $\beta$  are:

- stability of the calibration (temperature, radiation, ....)
- leakage effects (longitudinal and lateral)
- uniformity of the signal
- loss of energy in dead material
- ....

- $\gamma$  is the **noise term** (electronic noise,..)

- Also angular and spatial resolutions scale like  $1/\sqrt{E}$

Examples for energy resolutions seen in electromagnetic calorimeters in large detector systems:

Experiment	Calorimeter	$\alpha$	$\beta$	$\gamma$
L3	BGO	< 2.0%	0.3%	
BaBar	CsI (TI)	(*) 1.3%	2.1%	0.4 MeV
OPAL	Lead glass	(**) 5% (++) 3%		
NA48	Liquid krypton	3.2%	0.5%	125 MeV
UA2	Pb /Szintillator	15%	1.0%	
ALEPH	Pb / Prop.chamb.	18%	0.9%	
ZEUS	U / Szintillator	18%	1.0%	
H1	Pb / Liquid argon	11.0%	0.6%	154 MeV
D0	U / Liquid argon	15.7 %	0.3%	140 MeV

homogeneous  
calorimeters

sampling  
calorimeters

(\*) scaling according to  $E^{-1/4}$  rather than  $E^{-1/2}$

(\*\*) at 10 GeV

(++) at 45 GeV

## hadronic energy resolutions:

Experiment	Kalorimeter	$\alpha$	$\beta$	$\gamma$
ALEPH	Fe/Streamer Rohre	85%		-
ZEUS (*)	U/Szintillator	35%	2.0%	-
H1 (+)	Fe/Flüssig - Argon	51%	1.6%	900 MeV
D0	U/Flüssig - Argon	41%	3.2%	1380 MeV

(\*) compensating calorimeter

(+) weighting technique

- In general, the energy response of calorimeters is different for  $e/\gamma$  and hadrons; A measure of this is the so-called e/h ratio
- In so-called “compensating” calorimeters, one tries to compensate for the energy losses in hadronic showers ( $\rightarrow$  and bring e/h close to 1)

physical processes:

- energy recovery from nuclear fission, initiated by slow neutrons (uranium calorimeters)
- transfer energy from neutrons to protons (same mass) use hydrogen enriched materials / free protons

## 3.6 The ATLAS and CMS

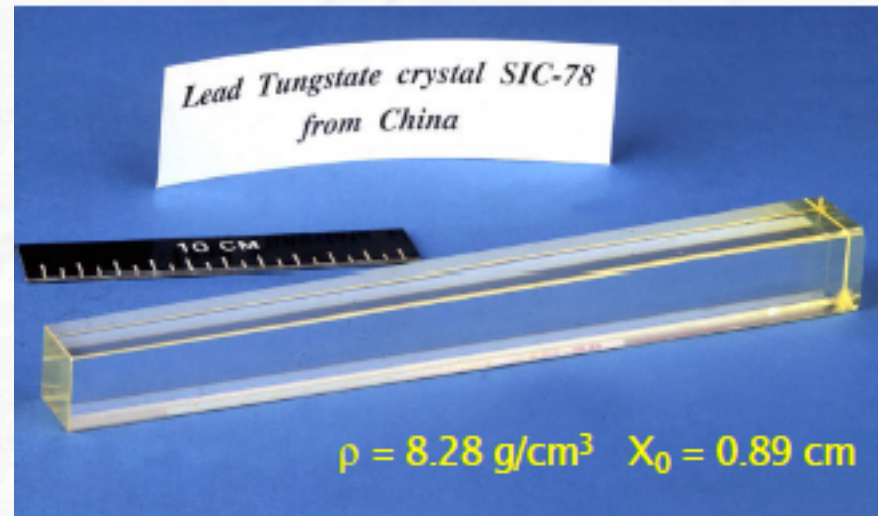
### calorimeters

CMS PbWO<sub>4</sub> crystal

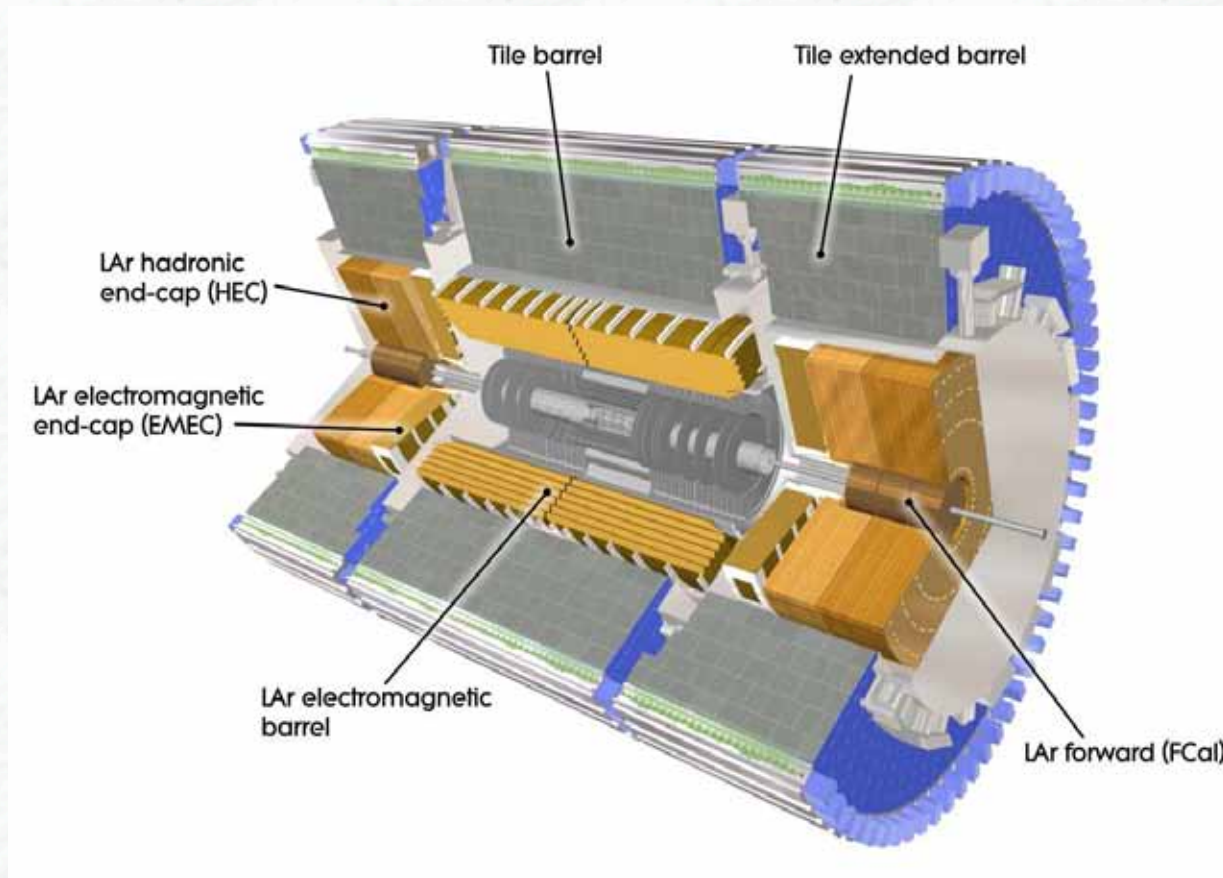
*Lead Tungstate crystal SIC-78  
from China*

10 CM

$\rho = 8.28 \text{ g/cm}^3$   $X_0 = 0.89 \text{ cm}$



# The ATLAS calorimeter system



- Liquid argon electromagnetic
- Liquid argon hadron calorimeter in the end-caps and forwards regions
- Scintillator tile hadron calorimeter in the barrel and extended end-cap region

# ATLAS and CMS electromagnetic calorimeters

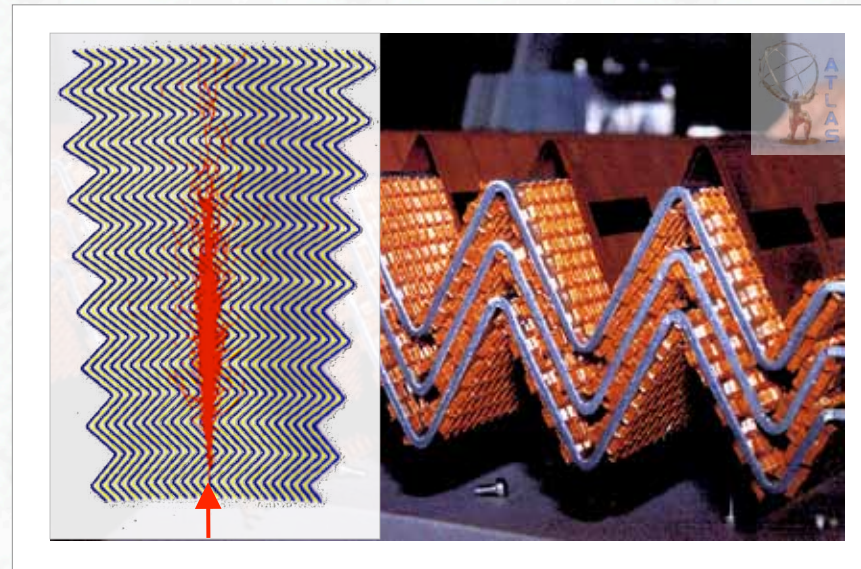
## ■ CMS: PbWO<sub>4</sub> Scint. Crystal Calorimeter

- Entire shower in active detector material
  - ▶ High density crystals ( $28 X_0$ )
  - ▶ Transparent, high light yield
  - ▶ No particles lost in passive absorber
  - ▶ High resolution:  $\sim 3\%/\sqrt{E}$  (stochastic)
- Granularity
  - ▶ Barrel:  $\Delta\eta \times \Delta\phi = 0.017^2$  rad
  - ▶ Longitudinal shower shape unmeasured

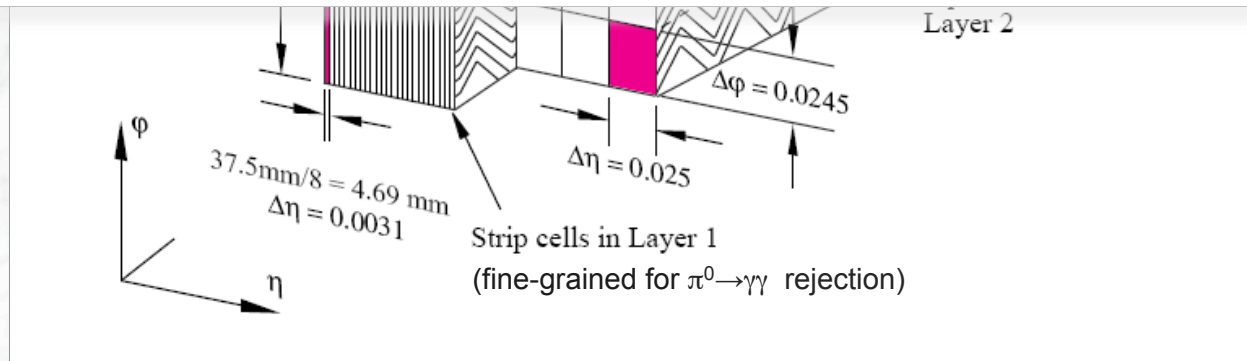
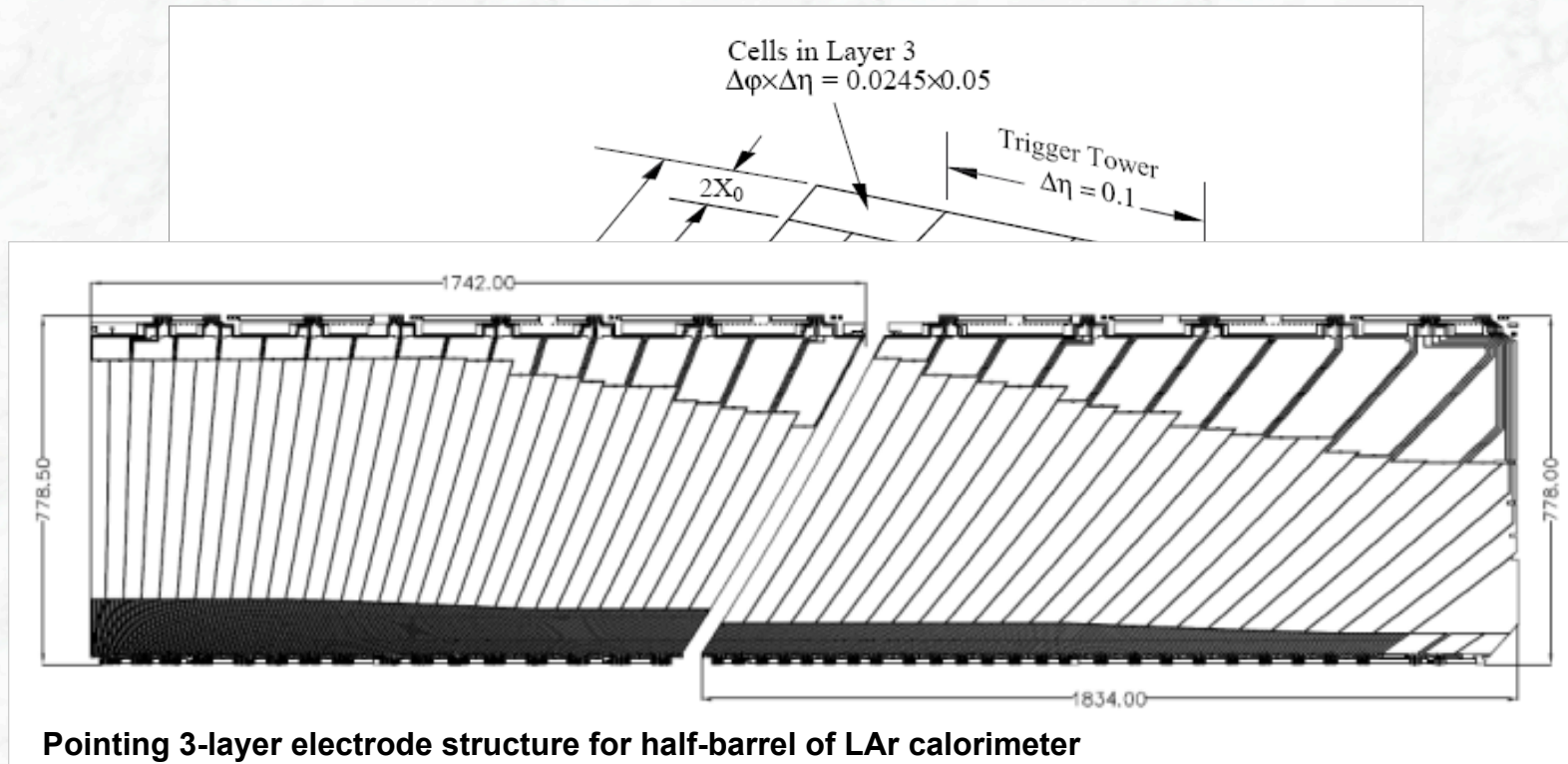


## ■ ATLAS: LAr Sampling Calorimeter

- Passive, heavy absorber (Pb, 1.1–1.5 mm thick [barrel]) inter-leaved with active detector material (liquid argon)
  - ▶ Overall  $22 X_0$
  - ▶ Accordion structure for full  $\phi$  coverage
  - ▶ Resolution:  $\sim 10\%/\sqrt{E}$  (stochastic)
- Granularity
  - ▶ Barrel:  $\Delta\eta \times \Delta\phi = 0.025^2$  rad (main layer)
  - ▶ Longitudinal segmentation (3 layers)

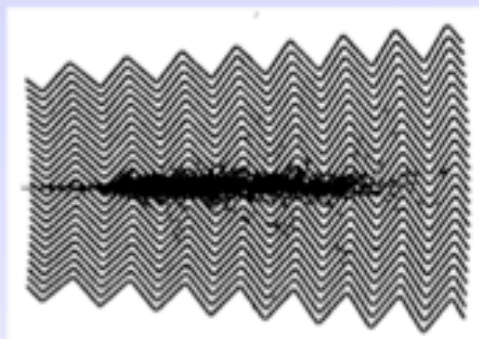


# ATLAS Liquid Argon EM Calorimeter



## ATLAS electromagnetic Calorimeter

Accordion geometry absorbers immersed in Liquid Argon



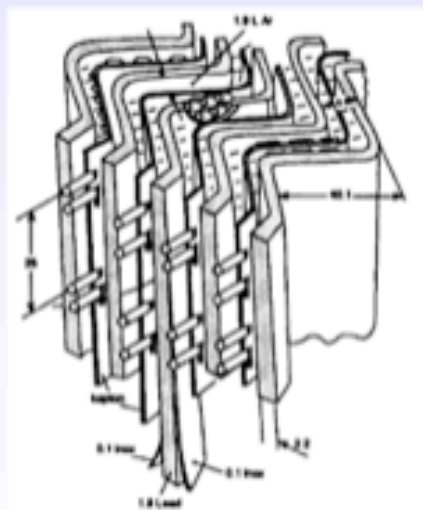
### Liquid Argon (90K)

+ lead-steel absorbers (1-2 mm)

+ multilayer copper-polyimide  
readout boards

→ Ionization chamber.

1 GeV E-deposit →  $5 \times 10^6 e^-$



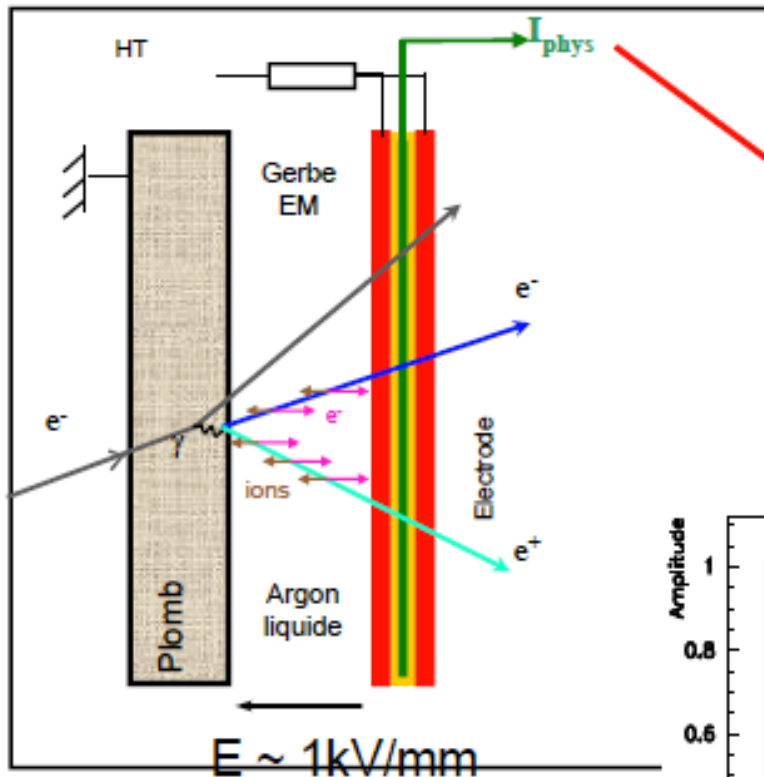
- Accordion geometry minimizes dead zones.
- Liquid Ar is intrinsically radiation hard.
- Readout board allows fine segmentation (azimuth, pseudo-rapidity and longitudinal) acc. to physics needs



Test beam results  $\sigma(E)/E = 9.24\%/\sqrt{E} \oplus 0.23\%$

Spatial resolution  $\approx 5 \text{ mm} / \sqrt{E}$

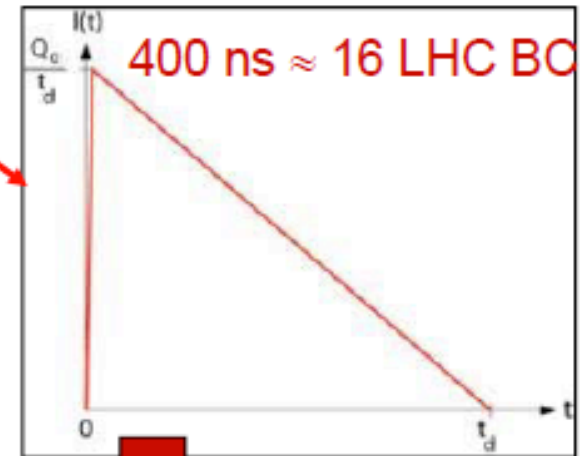
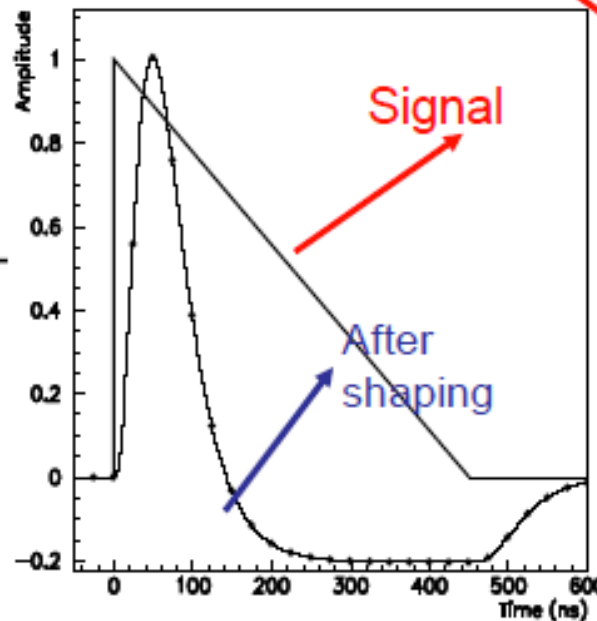
# Signal formation in a Liquid argon calorimeter and pulse shaping:



Signal is given from collection of released electrons

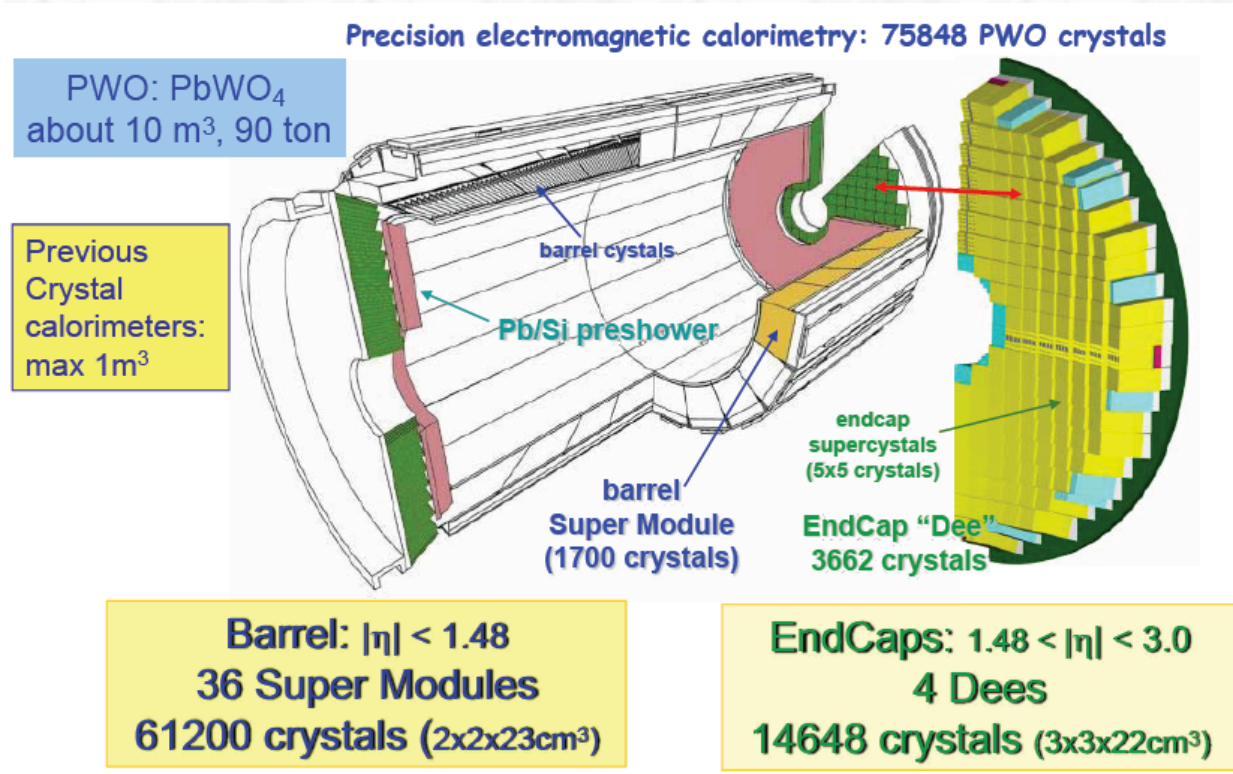
Drift velocity depends on electron mobility and applied field. In ATLAS :

LAr gap 2 mm,  $\Delta V = 2\text{kV}$



Instead of total charge (integrated current) measure the initial current  $I_0$ , (via electronic signal shaping), which is also proportional to the energy released

# The CMS calorimeter system



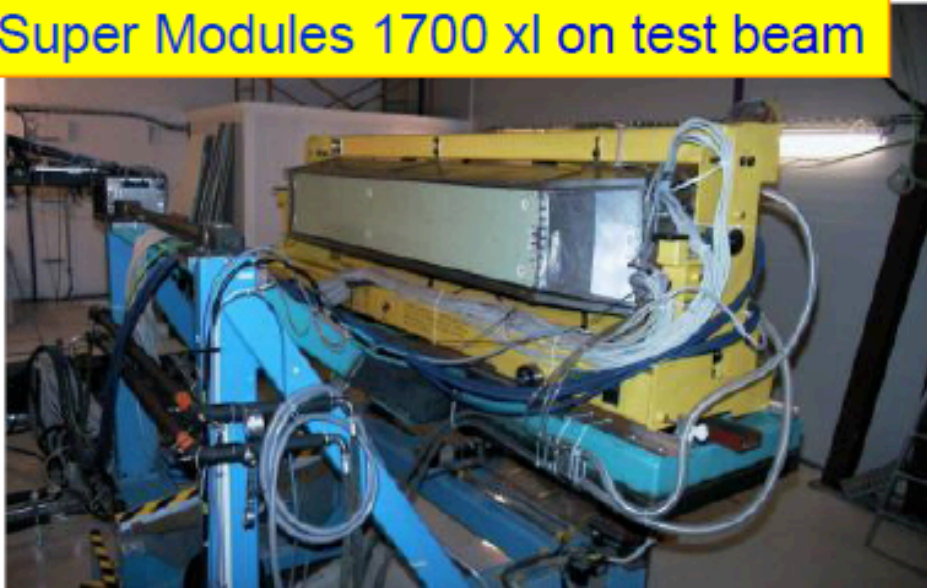
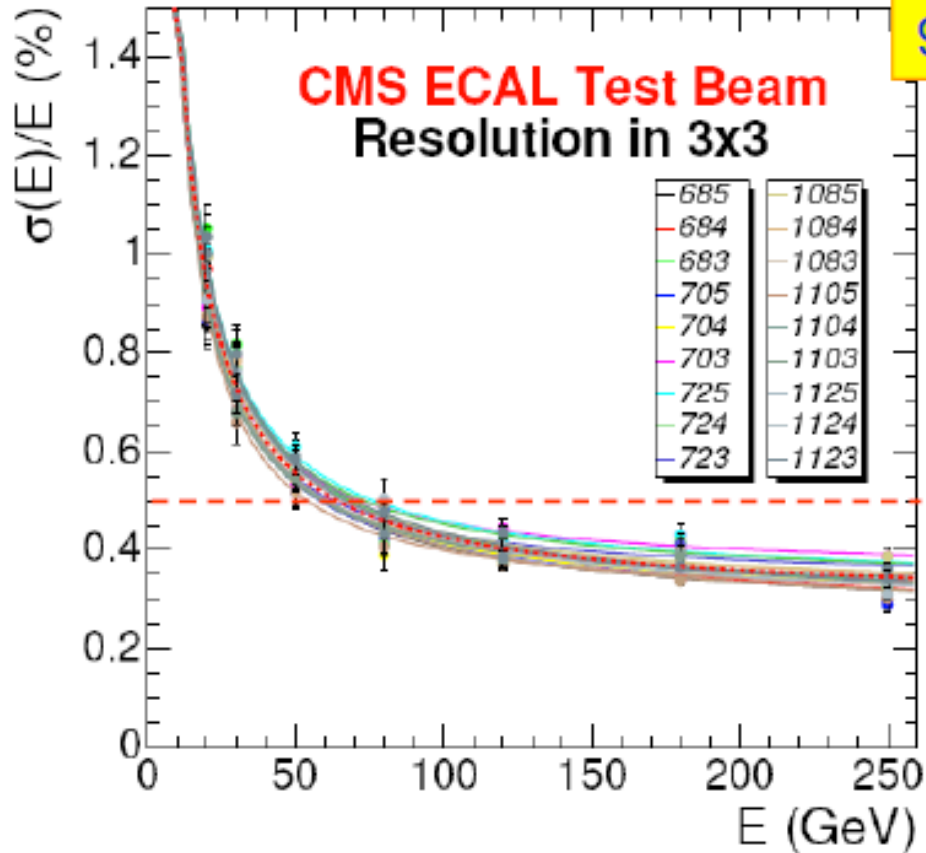
- $\text{PbWO}_4$  crystal  
el. magn calorimeter  
(homogeneous)
- Hadron calorimeter  
integrated in return yoke

# CMS el.magnetic calorimeter: crystal $\text{PbWO}_4$

Scintillator	Density [g/cm <sup>3</sup> ]	X <sub>0</sub> [cm]	Light Yield $\gamma/\text{MeV}$ (rel. yield*)	$\tau_1$ [ns]	$\lambda_1$ [nm]	Rad. Dam. [Gy]	Comments
NaI (Tl)	3.67	2.59	$4 \times 10^4$	230	415	$\geq 10$	hygroscopic, fragile
CsI (Tl)	4.51	1.86	$5 \times 10^4$ (0.49)	1005	565	$\geq 10$	Slightly hygroscopic
CSI pure	4.51	1.86	$4 \times 10^4$ (0.04)	10 36	310 310	$10^3$	Slightly hygroscopic
BaF <sub>2</sub>	4.87	2.03	$10^4$ (0.13)	0.6 620	220 310	$10^5$	
BGO	7.13	1.13	$8 \times 10^3$	300	480	10	
PbWO <sub>4</sub>	8.28	0.89	$\approx 100$	440 broad band 530 broad band		$10^4$	light yield =f(T)

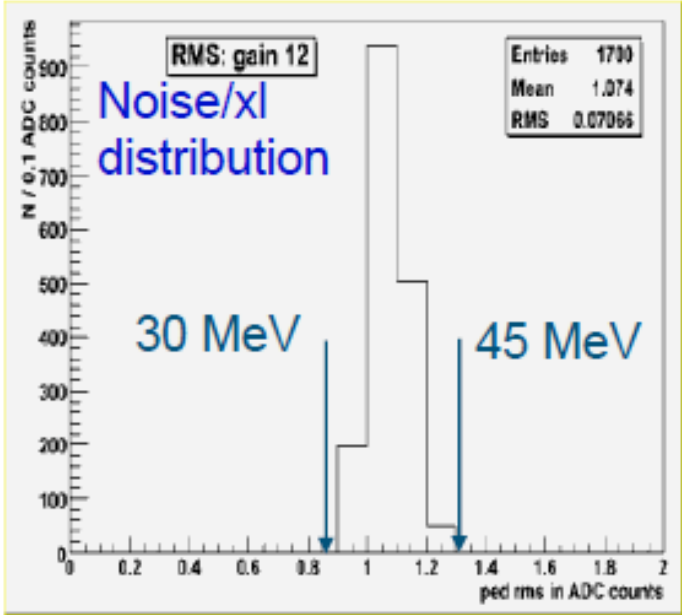


9 Super Modules 1700 xl on test beam



$$\frac{\sigma}{E} = \frac{2.8\%}{\sqrt{E(\text{GeV})}} \oplus \frac{125}{E(\text{MeV})} \oplus 0.3\%$$

Local resolution



# Comparison between ATLAS and CMS calorimeters

## CMS

Homogeneous calorimeter made of 75000  $\text{PbWO}_4$  scintillating crystals + PS FW

- Very compact  $R_M=2.0\text{cm}$
- Excellent energy resolution
- Fast  $\ll 100\text{ ns}$
- High granularity
- No longitudinal segmentation
- No angular measurement
- Radiation tolerance : needs follow up
- Room Temperature
- T sensitive  $5\%/^\circ\text{K}$
- Requires uniformisation by calibration

## ATLAS

Sampling LAr-Pb, 3 Longitudinal layers + PS

- $R_M=7.3\text{cm}$
- Good energy resolution
- Not so fast (450 ns), requires shaping
- High granularity
- Longitudinally segmented
- Angular measurement
- Radiation resistance
- Cryogenic detector (cryostat)
- T sensitive  $5\%/^\circ\text{K}$
- Intrinsically uniform

	ATLAS	CMS
EM calorimeter	Liquid argon + Pb absorbers $\sigma/E \approx 10\%/\sqrt{E} + 0.007$	$\text{PbWO}_4$ crystals $\sigma/E \approx 3\%/\sqrt{E} + 0.003$
Hadronic calorimeter	Fe + scintillator / Cu+LAr (10 $\lambda$ ) $\sigma/E \approx 50\%/\sqrt{E} + 0.03\text{ GeV}$	Brass + scintillator (7 $\lambda$ + catcher) $\sigma/E \approx 100\%/\sqrt{E} + 0.05\text{ GeV}$



# Muon Detectors

- Muon detectors are **tracking detectors** (e.g. wire chambers)
  - they form the outer shell of the (LHC) detectors
  - they are **not only sensitive to muons** (but to all charged particles)!
  - just by “definition”: if a particle has reached the muon detector, it's considered to be a muon (all other particles should have been absorbed in the calorimeters)

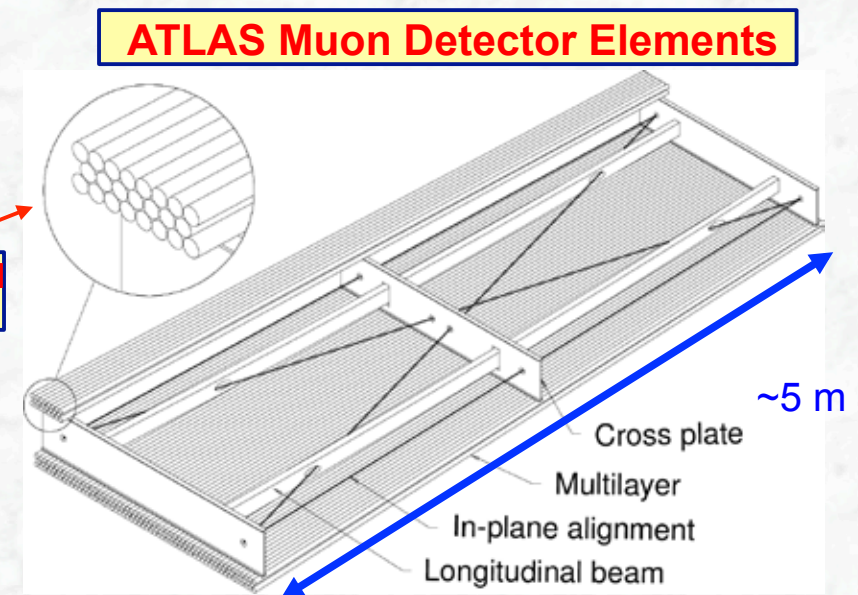
- Challenge for muon detectors

- large surface to cover (outer shell)
- keep mechanical positioning over time

- ATLAS

- 1200 chambers with 5500 m<sup>2</sup>
- also good knowledge of (inhomogeneous) magnetic field needed

**Aluminum tubes with central wire filled with 3 bar gas**



# ATLAS muon system

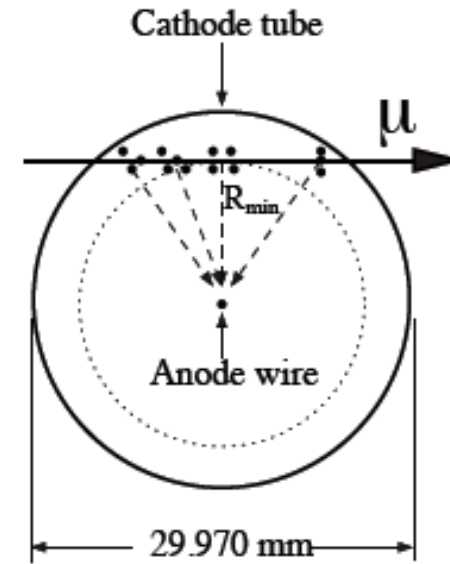
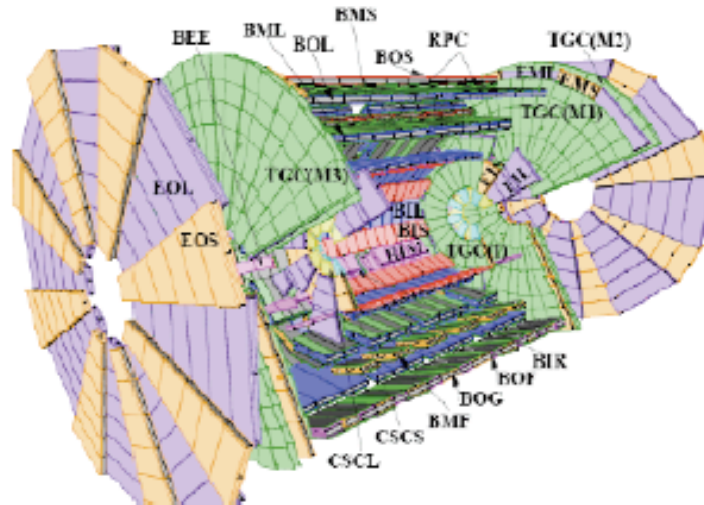
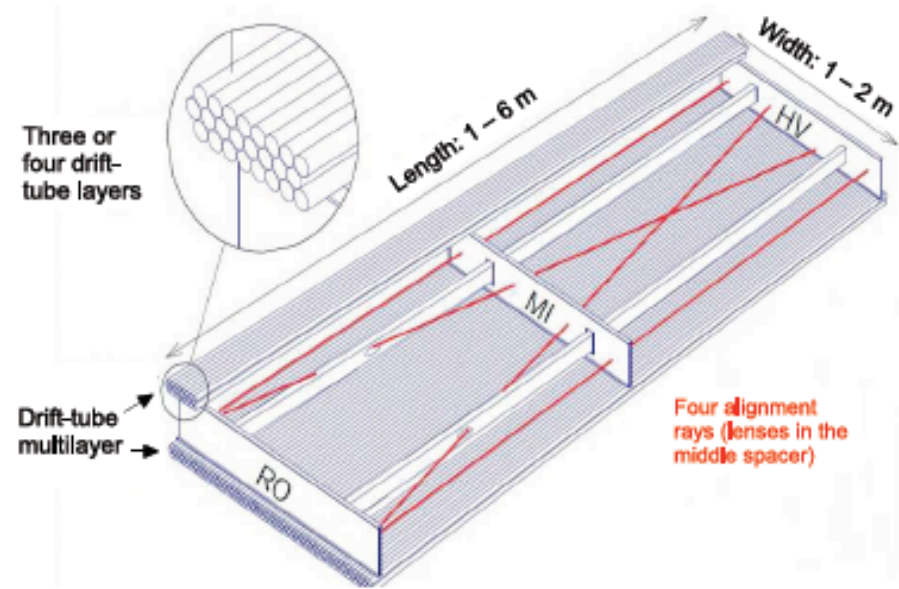
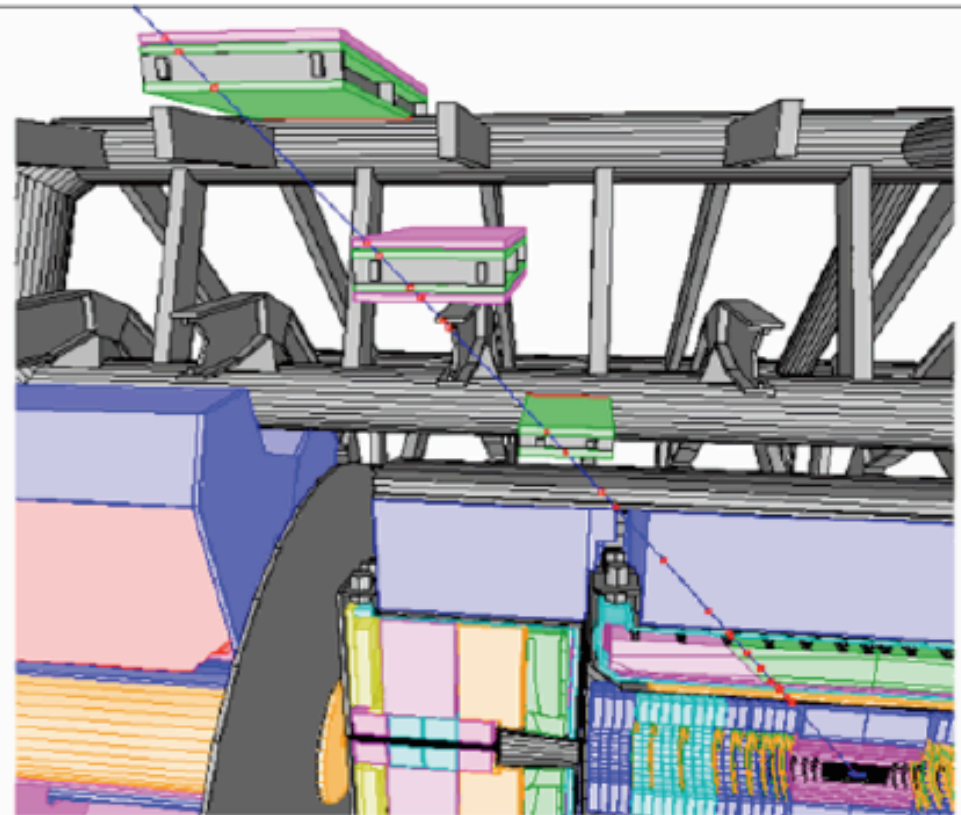
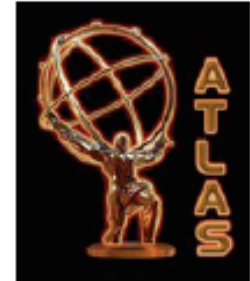
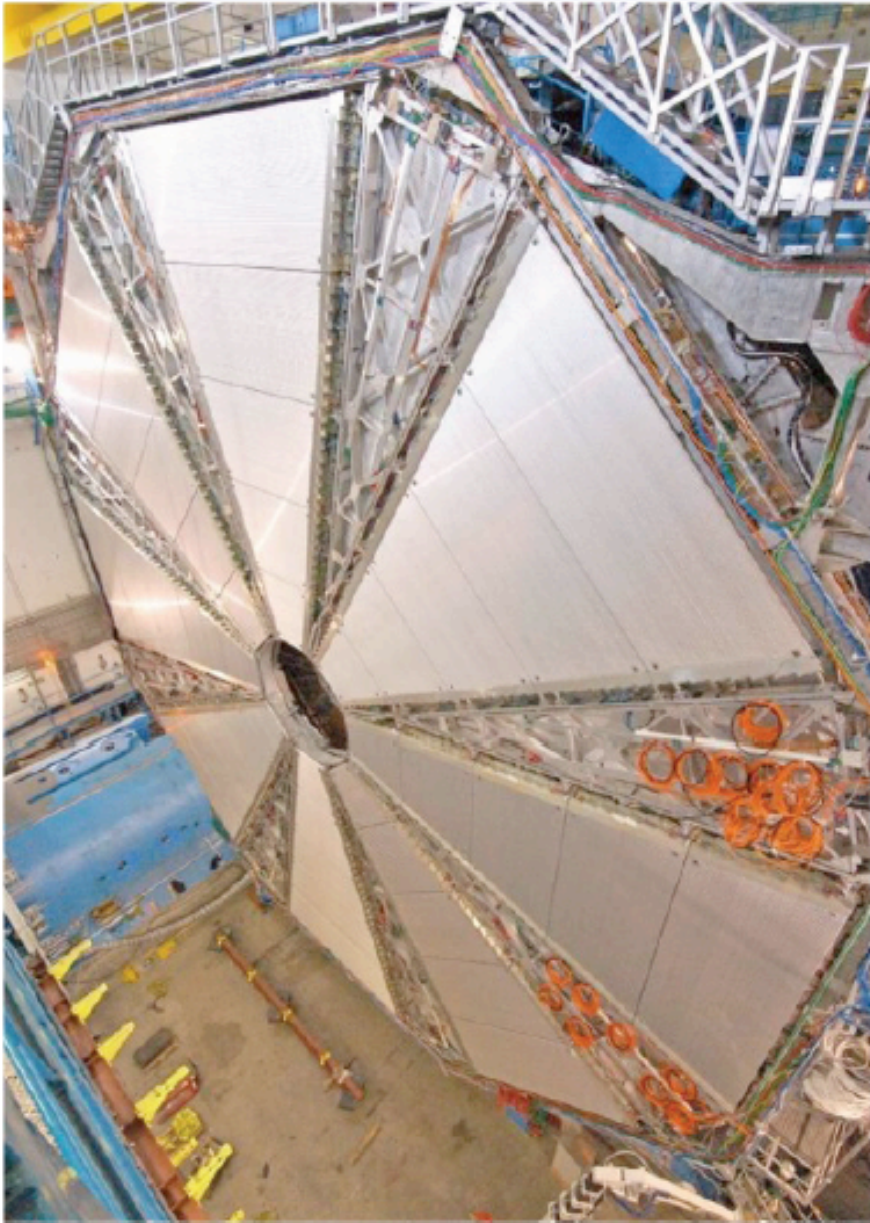


Table 6.2: Main MDT chamber parameters.

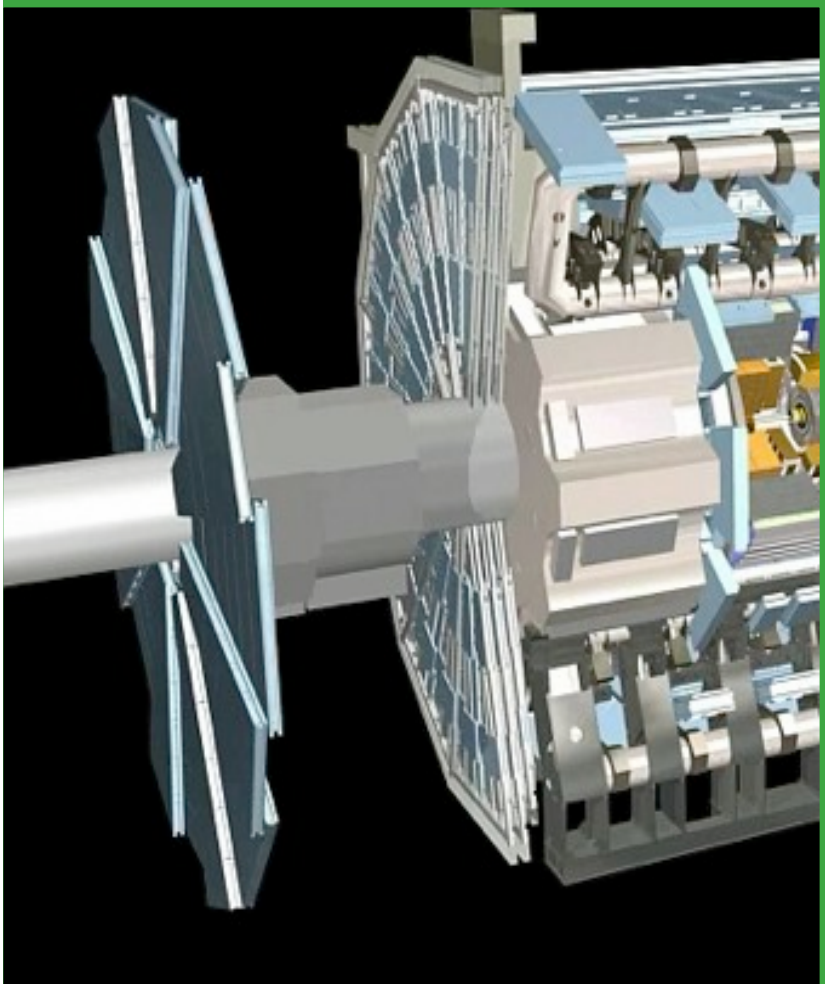
Parameter	Design value
Tube material	Al
Outer tube diameter	29.970 mm
Tube wall thickness	0.4 mm
Wire material	gold-plated W/Re (97/3)
Wire diameter	50 μm
Gas mixture	Ar/CO <sub>2</sub> /H <sub>2</sub> O (93/7/≤ 1000 ppm)
Gas pressure	3 bar (absolute)
Gas gain	2 x 10 <sup>4</sup>
Wire potential	3080 V
Maximum drift time	~ 700 ns
Average resolution per tube	~ 80 μm



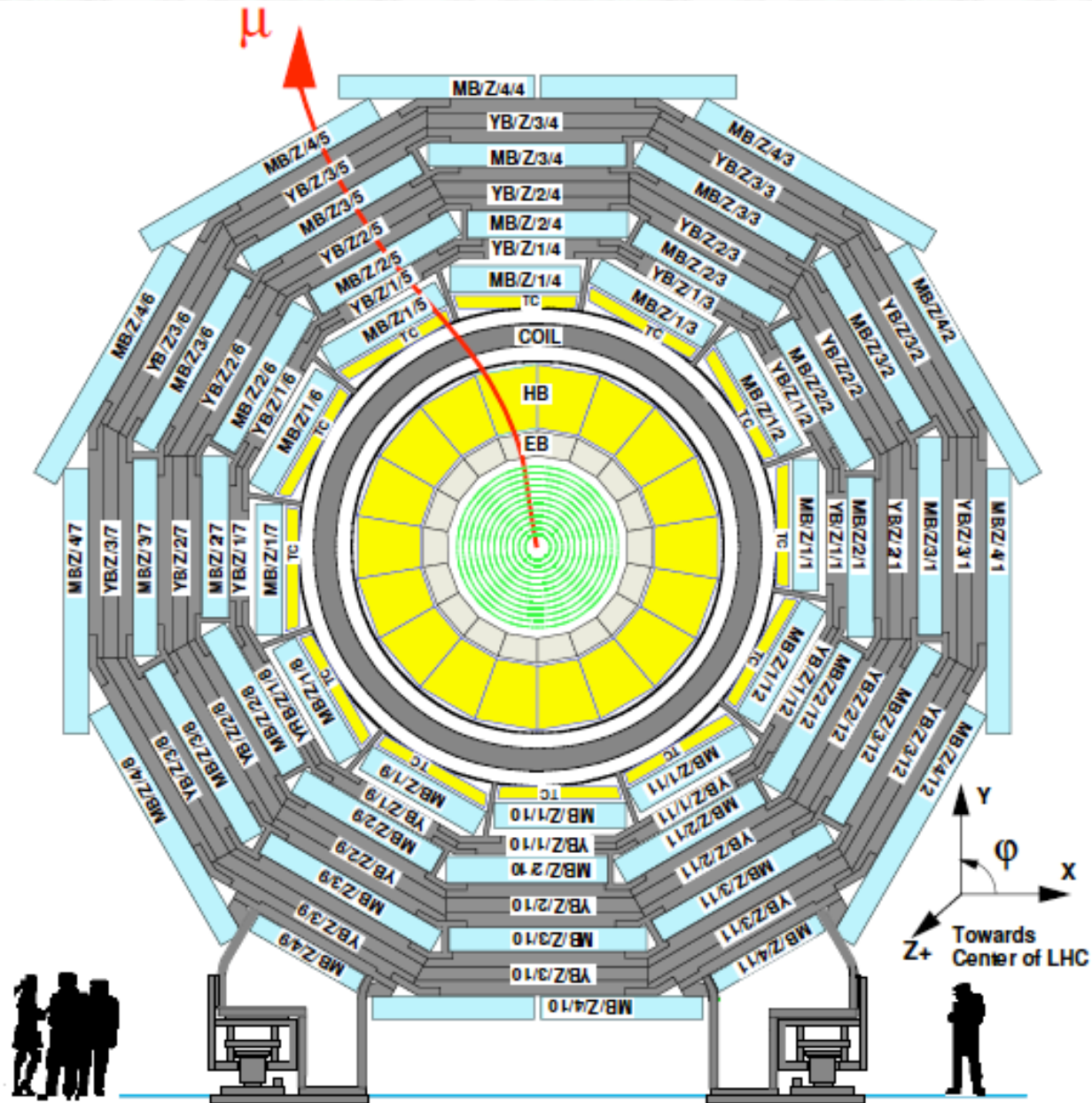
# ATLAS muon system



**Muon detector system  
In the forward region**



# CMS Muon system



# CMS

Superconducting  
Coil, 4 Tesla

## CALORIMETERS

### ECAL

76k scintillating  
PbWO4 crystals

### HCAL

Plastic scintillator/brass  
sandwich

IRON YOKE

## TRACKER

Pixels  
Silicon Microstrips  
210 m<sup>2</sup> of silicon sensors  
9.6M channels

## MUON BARREL

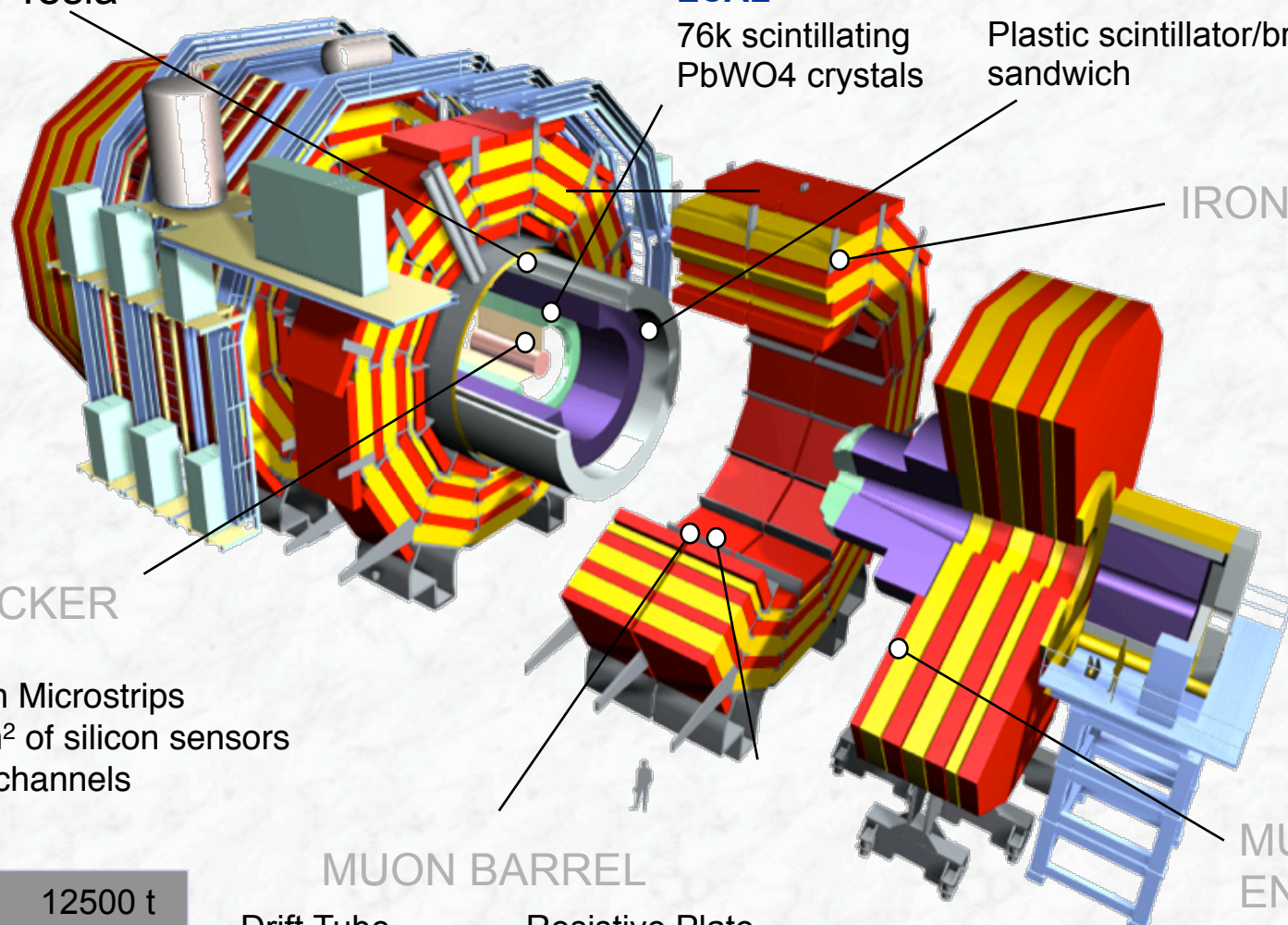
Drift Tube  
Chambers (**DT**)

Resistive Plate  
Chambers (**RPC**)

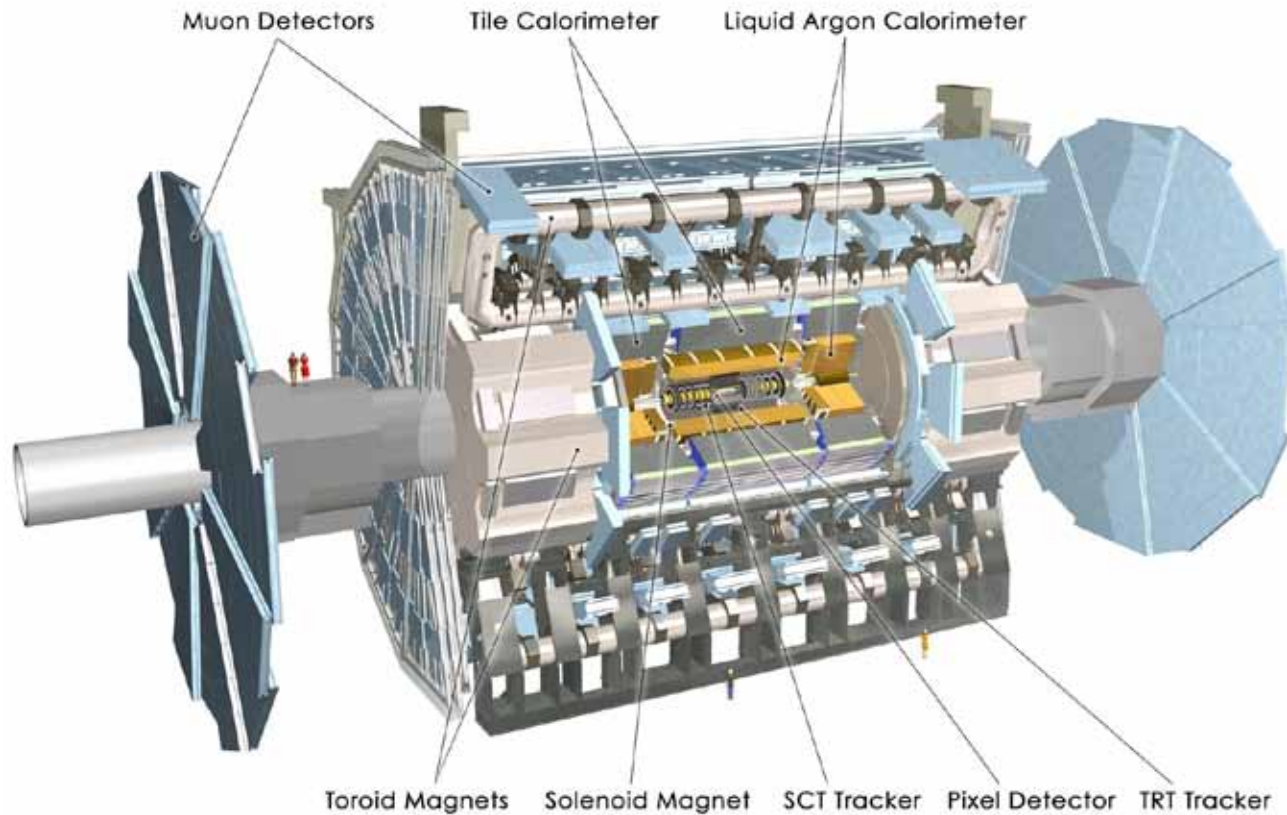
## MUON ENDCAPS

Cathode Strip Chambers (**CSC**)  
Resistive Plate Chambers (**RPC**)

Total weight	12500 t
Overall diameter	15 m
Overall length	21.6 m



## The ATLAS experiment



- Solenoidal magnetic field (2T) in the central region (momentum measurement)

High resolution silicon detectors:

- 6 Mio. channels (80  $\mu\text{m}$  x 12 cm)
  - 100 Mio. channels (50  $\mu\text{m}$  x 400  $\mu\text{m}$ )
- space resolution:  $\sim 15 \mu\text{m}$

- Energy measurement down to  $1^\circ$  to the beam line
- Independent muon spectrometer (supercond. toroid system)

Diameter	25 m
Barrel toroid length	26 m
End-cap end-wall chamber span	46 m
Overall weight	7000 Tons